Synthetic Metals 159 (2009) 541–545

Contents lists available at ScienceDirect

Synthetic Metals

journal homepage: www.elsevier.com/locate/synmet

Short communication

Electrochemical AFM investigation of horseradish peroxidase enzyme electro-immobilization with polypyrrole conducting polymer

Mohammed ElKaoutit[a,*], Ahmed Hosny Naggar[a,b], Ignacio Naranjo-Rodriguez[a], Manuel Dominguez[c], José Luis Hidalgo-Hidalgo de Cisneros[a]

[a] Departamento de Química Analítica, Facultad de Ciencias, Universidad de Cádiz, 11510 Puerto Real, Cádiz, Spain
[b] Chemistry Department, Faculty of Science, Al-Azhar University, Assiut Branch, 71524 Assiut, Egypt
[c] Departamento de Física de la Materia Condensada, Facultad de Ciencias, Universidad de Cádiz, 11510 Puerto Real, Cádiz, Spain

ARTICLE INFO

Article history:
Received 28 April 2008
Received in revised form 15 October 2008
Accepted 10 November 2008
Available online 6 January 2009

Keywords:
Electrochemical atomic force microscopy
conducting polymer
Horseradish peroxidase
Electro-immobilization

ABSTRACT

In this paper we investigate the nano-characterization of polypyrrole (Ppy) thin film electro-synthesized on highly oriented pyrolitic graphite (HOPG) with and without horseradish peroxidase enzyme (HRP) using Atomic force microscopy (AFM) performed in contact mode and fluid cell with electrolyte and potential control (ECAFM). *In situ* electro-synthesis of thin polypyrrole film was made by cyclic volt–amperommetry achieving structured Ppy nanoparticles with two types of particle sizes and the same ellipsoidal shape. Furthermore, the electro-immobilization of HRP, onto this film, was made at a fixed potential, achieving different morphology characterized by highly rough, non-homogeneous structure, and partial maintaining of the ellipsoidal particle in specific sites. The effect of polarization time on morphological parameters was studied and two mechanisms of electro-immobilization of HRP with Ppy conducting polymers were proposed.

1. Introduction

Since the birth of the first biosensor, thanks to the revolutionary work of Clark and Lyons, biosensor applications have seen an almost exponential increase in pharmaceutical, biotechnology, food, and other diverse areas such as green chemistry and bioenergy. Consequently, several groups have dedicated their efforts to achieve biosensors able to embrace the actual analytical challenges. One of the interesting lines of these efforts is the research of new materials or immobilization matrices and procedures capable to improve the stability, the biocatalytic sensitivity, and the selectivity of the biomolecules used in the desired biosensors. A good electrical conductivity, biocompatibility with biomolecule, accessibility, and chemical and physical inertias against the contacting solution can constitute basic criteria for the choice of materials for biomolecules immobilization. From a practical point of view, simplicity, repetitivity, instrumental control, possibility of miniaturization and automation of the fabrication procedure can represent additional conditions for this choice. Conducting polymers (CP) assure several of these conditions thanks to their obvious electrical conductivity, mechanical stability and the exclusive advantage of the controlled electro-synthesis which include the possibility of electro-immobilization of proteins as biological recognition element for biosensor making [1–10]. However, in spite of the undisputed advantages and interest of these polymers and also of the included electro-immobilization strategy in biosensor manufacturing, the mechanism of incorporation of the enzyme into the electro-synthesized polymer was not elucidated and has been object of various speculations [1]. Bartlett reported a mechanism based on electrostatic interactions between the polymer in its polycationic state and the negatively charged enzyme (i.e. above its isoelectric point) [3]. This mechanism has been extended up to the consideration of the negatively charged enzyme as a dopant species and also simulates the mechanism of electro-immobilization of proteins as that of the simple electro-synthesis of polymers [10]. The second mechanism is based on the "physical" entrapment of the protein in the electro-polymerized film, and explains the success of the method consisting in the deposition of the enzyme into a CP film followed by polarization of the electrode in a monomer solution [5]. Atomic force microscopy (AFM) probe may constitute an elegant opportunity to study the mechanism of electro-immobilization depending on the work conditions and procedure strategy. In this context, we present here preliminary results of electrochemical atomic force microscopy (ECAFM) study of the electro-synthesis of the Ppy and the electro-immobilization of the enzyme HRP with this conducting polymer onto highly oriented pyrolytic graphite (HOPG) surface. The choice of the HOPG as the surface, the Ppy as the CP, and the HRP as the protein can be justified by the high-crystalline order

* Corresponding author.
E-mail address: elkaoutit@uca.es (M. ElKaoutit).

0379-6779/$ – see front matter © 2008 Elsevier B.V. All rights reserved.
doi:10.1016/j.synthmet.2008.11.008

of the first, the most commonly usage of the second and because of the abundance and importance in the biosensor field of the third.

2. Materials and methods

Horseradish peroxidase (E.C.1.11.1.7, 269 U mg^{-1}) was purchased from Sigma (Steinheim, Germany), $LiClO_4$, for the supporting electrolyte, was from Fluka (Buchs, Switzerland), pyrrole monomer was from Sigma (Steinheim, Germany). Pure water was obtained by passing twice-distilled water through a Milli-Q system (18 MΩ cm, Millipore, Bedford, MA).

Voltammetric measurements were performed with an Autolab PGSTAT20 (Ecochemie, Ultrecht, The Netherlands) potentiostat/galvanostat interfaced with a personal computer, using the AutoLab software GPES for waveform generation and data acquisition and elaboration. In this article, electro-immobilization was carried out generally following the standard conditions established by Razolas et al. [11]. Also, we introduce the following modifications: the electrode used was glassy carbon (GCE), cleaned as described elsewhere [12], the scan rate was 50 mV s^{-1}, the monomer concentration (Ppy) was 5×10^{-5} mol L^{-1}, and the number of cycles was 5 in the potential range 0 to +1.6 V vs. Ag/AgCl, for Ppy prelayer. For Ppy-HRP layer, three scanning cycles from 0 to +1.0 V were applied in a 0.05 M $LiClO_4$ as supporting electrolyte containing 0.3 g L^{-1} of the enzyme and the same quantity of Ppy as in the prelayer step.

For scanning probe microscopy (SPM) studies, the highly oriented pyrolitic graphite (HOPG) was fixed on steel discs. The *in situ* ECAFM measurements were performed using a Veeco Nanoscope IIIa system, operated in contact mode with commercial Veeco oxidation-sharpened silicon nitride probes. ECAFM studies were made in the standard electrochemical cell with a Pt counter electrode and a Cu wire as reference electrode.

The prelayer was electrochemically synthesized on HOPG by *in situ* ECAFM. The electrolyte consisted of 5×10^{-5} mol L^{-1} Ppy and 0.1 mol L^{-1} $LiClO_4$. The potential was scanned from 0 to +1.6 V vs. Cu reference electrode. The Nanoscope cell for liquids, with a cell volume of approximately 0.15 mL and corresponding sample surface area of 56.00 ± 0.07 mm^2, was used. Thus, the thin Ppy film was synthesized and AFM image was registered in the same solution; then, the cell was emptied and solution containing 0.3 g L^{-1} of the enzyme was injected in the cell, and a potential of 0.5 V vs. Cu was applied for different time periods, while AFM images were registered after each period.

The roughness (R_a) is the arithmetic average of the absolute values of the surface height deviations measured from the mean plane within the scanned area. R_{max} is the height difference between the highest and lowest points on the surface relative to the mean plane. Surface area differences (S.A.D.) are the differences between the three-dimensional area of the image and its projected two-dimensional area. These parameters were extracted directly from roughness analysis carried out by the Nanoscope IIIa software [Nanoscope IIIa Version 5.12, Command Reference Manual (2002)]. The mean of R_a and S.A.D. data were given by

$$R_a = \frac{1}{n}\sum_{j=1}^{n}|Z_j|, \quad \text{S.A.D.} = \left[\frac{\sum(\text{surface area})_i}{\sum(\text{projected area})_i} - 1\right] \times 100$$

The size of grains was estimated from cross section profiles of the data along the reference line. The pair of cursors was positioned in horizontal and vertical lines to calculate the width and length of particles and the average was calculated from the corresponding population.

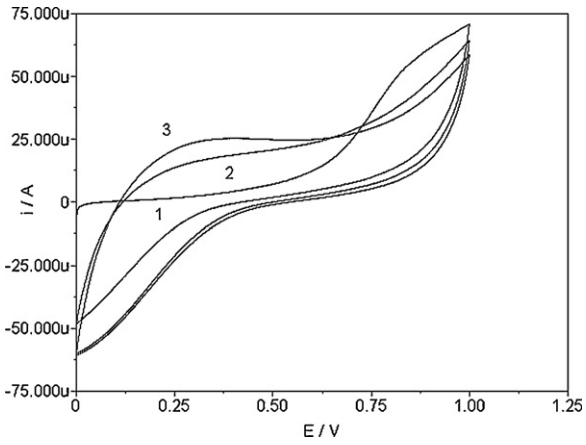

Fig. 1. Voltamogramms of electro-immobilization of HRP enzyme by Ppy in a conventional cell. Conditions are: 0.1 mol L^{-1} $LiClO_4$, 5×10^{-5} mol L^{-1} monomer and 0.3 g L^{-1} HRP, scan rate 50 mV s^{-1}.

3. Results and discussion

3.1. Cyclic voltammperometry of electro-immobilization

In the early cited paper [11] the effect of the number of cycles applied to electro-immobilized HRP enzyme with Ppy conducting polymer on the response of peroxide biosensor was studied and the authors concluded that the optimum response of the resulted biosensor was obtained for a layer elaborated by two cycles. On the other hand, other theoretical studies concluded that the thinnest layer includes the highest biochemical activity of the enzyme [13,14]. To investigate this fact, and get an experimental fundament for our contribution, conventional method was firstly used to investigate the electrochemical immobilization process. Cyclic voltammperomograms of the electro-immobilization process were registered and the result is presented in Fig. 1. It can be seen that, contrary to the reduction current, the oxidation current was increased by increasing the cycle number. For example, at a potential of 0.4 V this positive current has values of 25.6, 19.0, and 2.3 μA for 3, 2, and 1 cycle, respectively. This result can validate the mechanism of electro-immobilization based on the simulation of the enzyme as a dopant anion [10].

So, in the oxidation scan, the Ppy film was charged positively, and the enhancement of the current proved the incorporation of the enzyme nor in this step neither in the reduction phase. Consequently, and because of several operation limitations, the condition of the *in situ* ECAFM investigation of the enzyme electro-immobilization was carried out at a fixed potential equal to 0.5 V that is also useful to investigate the validity of this mechanism.

3.2. In situ AFM electro-synthesized Ppy nanoparticles thin film

Electrochemical AFM technique can constitute a powerful tool to study thin conducting polymer films. Usually, the morphological study of these materials was achieved by the usual techniques, such as SEM, TEM or AFM, but using samples early synthesized in a classical electrochemical cell, followed by manually removing and placing them into other surface for analysis. This procedure is limited by the film thickness and it is difficultly adaptable to study thin layers.

ECAFM was used to investigate the morphology of thin layer Ppy films, electro-synthesized on HOPG surface by the above described procedure and the result is presented in Fig. 2A. It can be seen that the formed film is very ordered, and the electropolymerization is initiated as individual particles with ellipsoidal

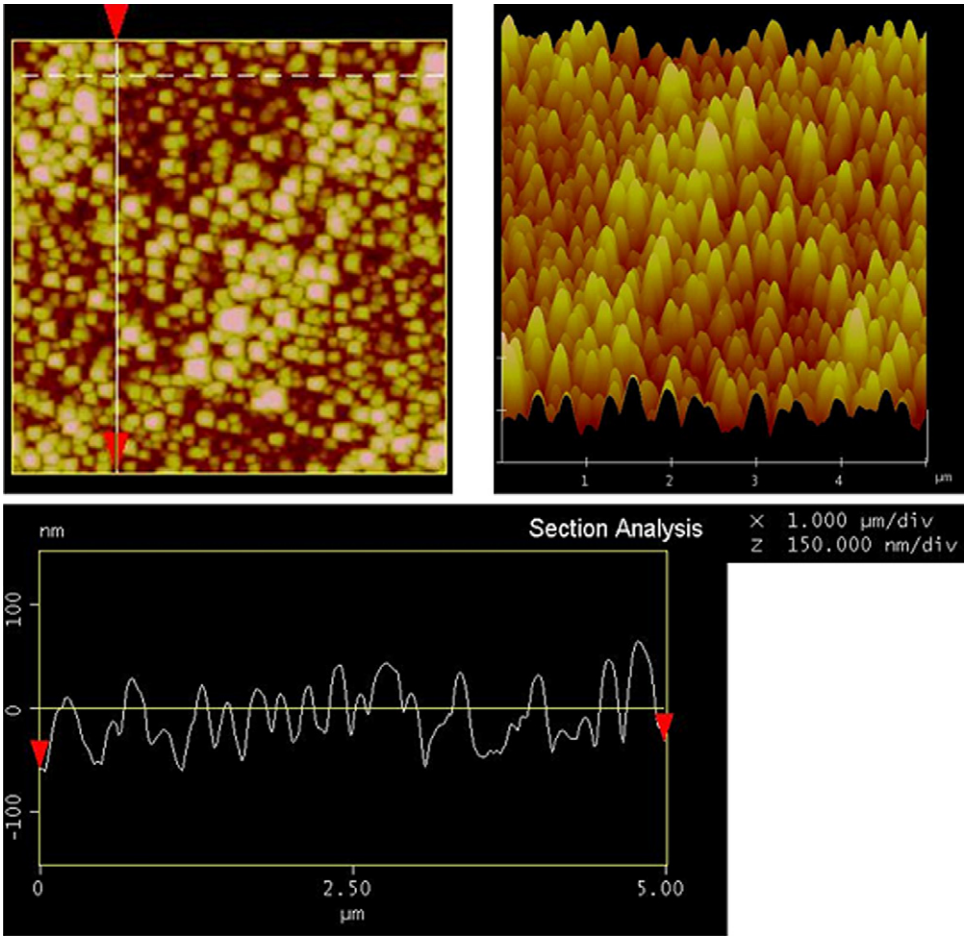

Fig. 2. ECAFM image of thin layer Ppy electro-synthesized on HOPG surface (A) and its analysis section (B). The potential was scanned from 0 to +1.6 V vs. Cu reference electrode with a scan rate of 100 mV s^{-1}; other chemical conditions as in Fig. 1.

shape and nucleation site from all HOPG surface. From section analysis, which is described in Fig. 2B, the dimension of these particles have been calculated, and the result can be described as two types of particles. The first has a width of 46.7 nm with a relative standard deviation (R.S.D.) of 42.8% and a length of 185.9 nm with R.S.D. of 17.8% (n = 115). The second having a width of 84.5 nm with R.S.D. 36.2% and a length of 295.5 nm with R.S.D. 15.1% (n = 54).

In addition, the same image was analyzed to calculate roughness parameters and surface area differences as described in Section 2, and the results are summarized in Table 1. It is interesting to note that the two particle types showed are very small, more than those observed for Ppy nanowires electro-polymerized within poly(methyl methacrylate) nanochannels on an indium tin oxide substrate [15], and that Ppy or Ppy-silicate biologically [16] or chemically [17] synthesized. This can be explained by the highest orientation of HOPG substrate and the operational conditions.

Table 1
Roughness parameters of Ppy prelayer, Ppy-HRP electro-synthesized with 60 s as polarization time and that with 315 s [*pt: polarization time, for parameters meaning, see Section 2].

Sample	R_a (nm)	R_{max} (µm)	S.A.D. (%)
Ppy prelayer	23.0	0.303	23.3
Ppy-HRP (pt* = 60.5 s)	232.7	2.322	33.3
Ppy-HRP (pt = 315.5 s)	204.7	1.532	27.0

3.3. Investigation of enzyme electro-immobilization

The morphology of the enzyme electro-immobilized in polypyrrol film was also studied by AFM in contact mode. Several films were electro-synthesized at 0.5 V vs. Cu varying the polarization time parameter. Fig. 3, shows the topography of those elaborated by 60 s (A), and 315 s (B). There are several differences between these two images and that of nano-structured Ppy in Fig. 2A. The most important novelty is the appearance of great homogeneous blocks embedded in the same ellipsoidal small structure seen in Fig. 2, and attributed to *Ppy* nanoparticles. In addition, in Fig. 3A, these blocks show a laminar structure which remind us the crystalline structure of commercial HRP. It is difficult to demonstrate this remark. Thus, the usual techniques used are FTIR or XRD, these techniques are known by their lower sensitivity and an adequate quantity of the immobilized enzyme is required for its conformational or crystallographic study. We have tried to follow this line but unfortunately, no signal attributed to the polypeptide was registered, even using a sum of up to 10 electro-synthesized films. However, various works have studied the morphology of Ppy and reported that the *Ppy* surface has a continuous structure with a rough and cauliflower-like shape [18–23]. Thus, we can consider these blocks as crystallized HRP. Assuming this and remarking these two images, we can conclude that these crystals are clearly seen embedded in the polypyrrole matrix. This embedment is improved with the increase of polymerization time. The morphological parameters of these films were calculated and the results are summarized in Table 1. These parameters were directly calcu-

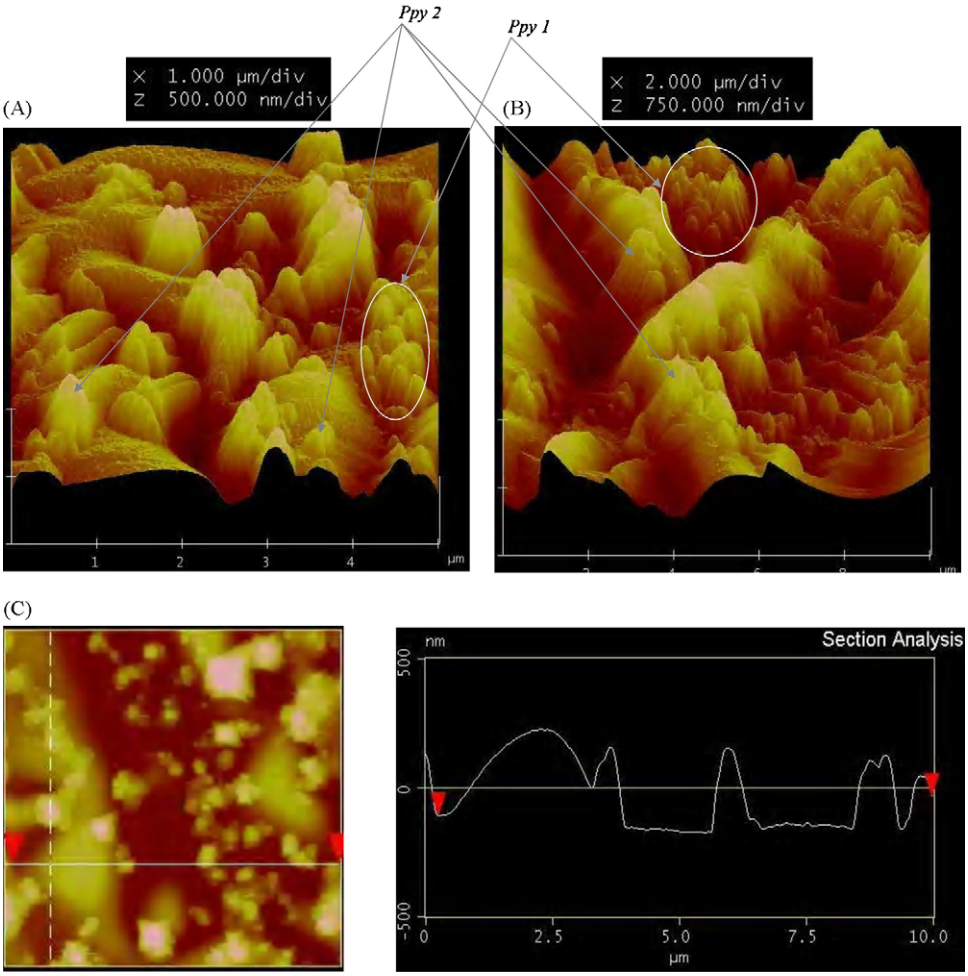

Fig. 3. ECAFM images of HRP electro-immobilized by Ppy at fixed 0.5 V vs. Cu potential, during 60 s (A), 350 s (B), and typical section analysis of these films (C). Enzyme concentration is 0.3 g L^{-1} and other chemical conditions are as in Figs. 1 and 2.

lated from captured images (5 μm × 5 μm) without any treatments (flatten and smoothing). Non-proportionality of the roughness parameters with the time of the polarization can be concluded. Also, we can note an important decrease in R_{max} (and consequently in R_a) comparing these samples. They can be attributed to a simultaneous increase of both Ppy nanoparticles and HRP crystals and it is in accordance with other study, in which an inverse effect of the polarization time on the sensitivity of the Ppy-HRP or Ppy-glucose oxidase based biosensors was concluded [11,24].

Section analysis of these images (Fig. 3C) reveals two types of particles, having similar shape to those observed in Ppy thin layer, but with different growing site. The first one grows from a relative planar surface. The second one grows from or near the block structure attributed to the crystallized enzyme. We can confirm that they are two nucleation sites for electro-polymerization of Ppy in the presence of HRP; the normal one, from the electrode surface, and that from the crystallized enzyme. In Fig. 3, we can clearly distinct between these two types of nucleation sites, *Ppy-1* as a notably agglomeration structure of nano-ellipsoidal shape, and *Ppy-2* as individual or few agglomerated ellipsoidal particle (see Fig. 3A and B).

From this, we can suggest two mechanisms of electro-immobilization. The first is purely physical and consists in the growth of the Ppy chains in the intimate contact of the HRP block crystals. The second is based on the charges difference of the components; the particles, beginning their formation from the block, prove that the Ppy as well as the oxidized species of pyrrole can be adsorbed on the enzyme periphery and start a new polymerization chain from this enzyme site. The two proposed mechanisms, embedment and formation of Ppy film into the crystallized enzyme are in accordance with theoretical and experimental studies of the effect of polarization on the biosensors response [11,13,14,24] so the formation of Ppy barrier diffusion of the substrate from the solution to catalytic site of the enzyme should be a result of an excess in a polarization time.

4. Conclusion

In this article, we have initiated a new line to investigate the highly interesting procedure of enzyme electro-immobilization. We report topographic images of the electro-synthesis of Ppy with and without HRP, at nanoscale and with high resolution. Initial tentative to detail the mechanisms of electro-immobilization was carried out. It can be concluded that the mechanism can be the physical entrapment as well as the adsorption followed by crystallization of the enzyme on and into the Ppy film. In the presence of enzyme, the growth of CP film keeps a similar ellipsoidal shape to that observed without the biomolecule, and can take place at the peripheral surface of the crystallized enzyme. This result proves the importance of the enzyme charge in the process and similar studies varying the pH of the medium can constitute a perspective of this work.

References

[1] T. Ahuja, I.A. Mir, D. Kumar, Rajech, Biomaterials 28 (2007) 791.
[2] P.N. Bartlett, P.R. Birkin, Synth. Met. 61 (1993) 15.
[3] P.N. Bartlett, J.M. Cooper, J. Electroanal. Chem. 362 (1993) 1.
[4] G. Bidan, Sens. Actuat. B: Chem. 6 (1992) 45.
[5] S. Cosnier, Biosens. Bioelectron. 14 (1999) 443.
[6] S. Cosnier, Anal. Bioanal. Chem. 377 (2003) 507.
[7] M. Gerard, A. Chauby, B.D. Malhotra, Biosens. Bioelectron. 17 (2002) 345.
[8] M.V. Deshpande, D.P. Amalnerkar, Prog. Polym. Sci. 18 (1993) 623.
[9] B.D. Malhotra, A. Chaubey, S.P. Singh, Anal. Chim. Acta 578 (2006) 56.
[10] J.-C. Vidal, E. Garcia-Ruiz, J.-R. Castillo, Microchim. Acta 143 (2003) 93.
[11] S.S. Razola, B.L. Ruiz, N.M. Diez Jr., H.B. Mark, J.-M. Kauffmann, Biosens. Bioelectron. 17 (2002) 921.
[12] M. El Kaoutit, D. Bouchta, H. Zejli, N. Izaoumen, K.R. Temsamani, Anal. Lett. 37 (2004) 1671.
[13] M.D. Mell, J.T. Maloy, Anal. Chem. 47 (1975) 299.
[14] P.N. Bartlett, R.G. Whitaker, J. Electroanal. Chem. 224 (1987) 27.
[15] J.-M. Chen, S.-W. Liao, Y.-C. Tsai, Synth. Met. 155 (2005) 11.
[16] A. Ramanaviciene, W. Schuhmann, A. Ramanavicius, Colloids Surf. B: Biointerf. 48 (2006) 159.
[17] A. Azioune, A. Ben Slimane, L. Ait Hamou, A. Pleuvy, M.M. Chehimi, C. Perruchot, S.P. Armes, Langmuir 20 (2004) 3350.
[18] N. Izaoumen, D. Bouchta, H. Zejli, M. El Kaoutit, A.M. Stalcup, K.R. Temsamani, Talanta 66 (2005) 111.
[19] K. Yamamoto, Y.S. Park, S. Takeoka, E. Tsuchida, J. Electroanal. Chem. 318 (1991) 171.
[20] G. Chander, D.K. Pletcher, J. Appl. Electrochem. 16 (1986) 62.
[21] W. Chen, C.M. Li, P. Chen, C.Q. Sun, Electrochim. Acta 52 (2007) 2845.
[22] M.F. Suárez, R.G. Compton, J. Electroanal. Chem. 462 (1999) 211.9.
[23] F.T.A. Vork, B.C.A.M. Schnermans, E. Barendrecht, Electrochim. Acta 35 (1990) 567.
[24] D.R. Yaniv, L. McCormick, J. Wang, N. Naser, J. Electroanal. Chem. 314 (1991) 353–361.